

Negative magnetoresistance temperature dependence induced by current-pumped nuclear spin polarization at the $\nu = \frac{2}{3}$ quantum Hall state

Shibun Tsuda,^{1,*} Minh-Hai Nguyen,^{1,†} Daiju Terasawa,² Akira Fukuda,² and Anju Sawada³

¹*Department of Physics, Graduate School of Science, Kyoto University, Kyoto 606-8502, Japan*

²*Department of Physics, Hyogo College of Medicine, Nishinomiya 663-8501, Japan*

³*Research Center for Low Temperature and Materials Sciences, Kyoto University, Kyoto 606-8501, Japan*

(Received 31 May 2015; revised manuscript received 2 February 2016; published 22 March 2016)

We investigate the huge longitudinal resistance (HLR) at which the magnetoresistance of the $\nu = \frac{2}{3}$ fractional quantum Hall state (QHS) is increased with dynamic nuclear spin polarization. We measure the magnetoresistance temperature dependence in the resistively saturated HLR by increasing the temperature of the sample rapidly in order to prevent relaxation of the nuclear spin polarization. The obtained results indicate that the magnetoresistance decreases as the temperature increases. The Hall resistance in the HLR is also measured and found to exhibit a plateau close to a quantized value. We discuss the negative magnetoresistance temperature dependence with a stripe-shaped domain state deformed by the nuclear spin polarization.

DOI: [10.1103/PhysRevB.93.125426](https://doi.org/10.1103/PhysRevB.93.125426)

I. INTRODUCTION

Under a high magnetic field at low temperature, a two-dimensional electron system (2DES) exhibits fractional quantum Hall states (FQHSs). The FQHSs show not only a variety of phenomena originating from Coulomb interactions, but also spin-related phenomena due to the spin degree of freedom [1,2]. For example, the quantum Hall state (QHS) with filling factor $\nu = \frac{2}{3}$ has two ground states with different spin polarizations [3]. At the spin phase transition point of the $\nu = \frac{2}{3}$ QHS, a huge longitudinal resistance (HLR) with hysteretic transport has been observed by Kronmüller *et al.* [4]. In addition, rf-irradiation experiments involving the nuclear magnetic resonance (NMR) frequencies of Ga and As atoms in a quantum well have shown that nuclear spin polarization (NSP) is the origin of the magnetoresistance R_{xx} peak [5]. A relaxation measurement conducted by Hashimoto *et al.* [6] has suggested that the R_{xx} enhancement at the $\nu = \frac{2}{3}$ QHS reflects the degree of NSP. Resistively detected NMR and relaxation measurements have since developed as highly effective techniques for the study of the spin states of various exotic QHSs, such as the Goldstone mode of the skyrmion lattice near the $\nu = 1$ QHS [6], the canted antiferromagnetic phase in the bilayer $\nu = 2$ QHS [7], and the spin polarization in the even-denominator fractional $\nu = \frac{5}{2}$ non-Abelian QHS [8].

Thus far, the mechanism of the R_{xx} enhancement has been understood as follows: At the spin transition point, two FQHSs with different spin polarizations degenerate energetically according to the composite Fermion model [3,9] and domain structures are formed [4,10,11]. It is believed that the electron spins are flipped when a current passes across the domain boundaries, and simultaneously, the electron spin flips cause nuclear spin flips. This flip-flop process results in dynamic nuclear spin polarization (DNSP), which in turn affects the domain formation and increases the lengths of the domain

boundaries [10,11]. In addition, an anisotropy in the hysteretic transport has been observed for the angle between the current direction and the in-plane magnetic field around the transition point [12]. This suggests that the dynamics of quantum Hall domains is affected by the current direction relative to the in-plane field. However, details of the domain structure are still unclear, and the actual mechanism of the R_{xx} enhancement remains uncertain.

A previous experiment has shown that the HLR is unstable and decays over a period of roughly several hundred seconds [12]. In this work the resistance measurement is performed significantly faster than the HLR decay time. Also, to avoid the heating effect of the current, we use a sufficiently small measuring current value after DNSP has been achieved by current pumping with a large current of 60 nA. Furthermore, we measure the temperature dependence of the R_{xx} of the HLR within a short period of several tens of seconds. With this method we find that the R_{xx} of the HLR has a negative temperature dependence. By investigating R_{xx} and the Hall resistance R_{xy} in the HLR as a function of ν , the HLR is found to exhibit an almost quantized R_{xy} plateau. We discuss both the negative temperature dependence of R_{xx} and the R_{xy} plateau using a stripe-shaped domain model. The outline of the paper is as follows. Section II describes the experimental setup and sample characterization. The measurement procedures and results are detailed in Sec. III. Finally, we discuss possibilities regarding the HLR state in Sec. IV.

II. EXPERIMENTAL SETUP AND SAMPLE

The sample employed in our experiments consists of two 20-nm-thick GaAs/AlGaAs quantum wells processed into a 50- μm -wide Hall bar with a voltage probe distance of 180 μm . The sample was previously used for an experiment on interlayer diffusion of nuclear spins [13]. The unique structure of the sample is that modulation doping is performed on the front layer only, and the back-layer electrons are fully field induced through an n^+ -GaAs layer acting as a back gate [14]. We use the front layer and deplete electrons from the back layer. The electron density n is controlled by the gate voltage,

*shibun@sphys.kyoto-u.ac.jp

†Present address: Department of Physics, Cornell University, Ithaca, New York 14853.

and the low-temperature mobility is $2.2 \times 10^6 \text{ cm}^2/\text{V s}$ with $n = 2.0 \times 10^{11} \text{ cm}^{-2}$. The sample is placed inside a mixing chamber filled with liquid helium in a dilution refrigerator with a base temperature of 66 mK. We measure R_{xx} and R_{xy} using a standard low-frequency ac lock-in technique at a frequency of 37.7 Hz. The magnetic field is applied by a superconducting magnet with a maximum field of 13.5 T. Measurements are performed at 7.19 T, at which value the phase transition between the spin unpolarized and polarized states occurs at exactly the $\nu = \frac{2}{3}$ point. A RuO_2 resistor calibrated in the magnetic field is used as a thermometer, and a heater is placed at a distance of 1 cm from the sample immersed in the liquid helium of the mixing chamber.

III. MEASUREMENTS AND RESULTS

A. Temperature dependence

Figure 1(a) shows the R_{xx} in the vicinity of the $\nu = \frac{2}{3}$ unpolarized QHS at 6.4 T, which indicates a sufficiently developed QHS. As the spin phase transition of the $\nu = \frac{2}{3}$ QHS does not realize at this field, a hysteresis phenomenon is not observed. Next, we increase the magnetic field to 7.19 T

so as to realize the phase transition from the unpolarized phase to the polarized phase. The R_{xx} bump at the spin phase transition point [indicated by the upwards-pointing arrow of Fig. 1(b)] is clearly observed. We can identify remarkable hysteresis through measurement of the various current and sweep directions. The hysteresis of a large current of 30 nA can be observed around the spin transition point with slow sweeping of ν . The hysteretic behavior of a small current of 5 nA is much smaller than that of 30 nA. These results are similar to previous reports [10,15,16]. At $\nu = 0.65$ [the broken straight line in Fig. 1(b)], we perform DNSP with a 60 nA current for 1800 s. By pumping NSP, R_{xx} increases for approximately 500 s and saturates [the red triangles in Fig. 1(c)]. After pumping, with a sudden change in the measuring current to a small value of 1 nA to prevent the self-heating effect, R_{xx} is enhanced by a factor of 2 [the blue square in Fig. 1(c)]. We have experimented with DNSP at various ν and found that the enhancement of R_{xx} from the initial value is largest at $\nu = 0.65$; therefore, we pump NSP at this value in later measurements.

To investigate the temperature dependence of R_{xx} in the HLR, we increase the temperature of the mixing chamber containing the sample by supplying heat for 50 s after the

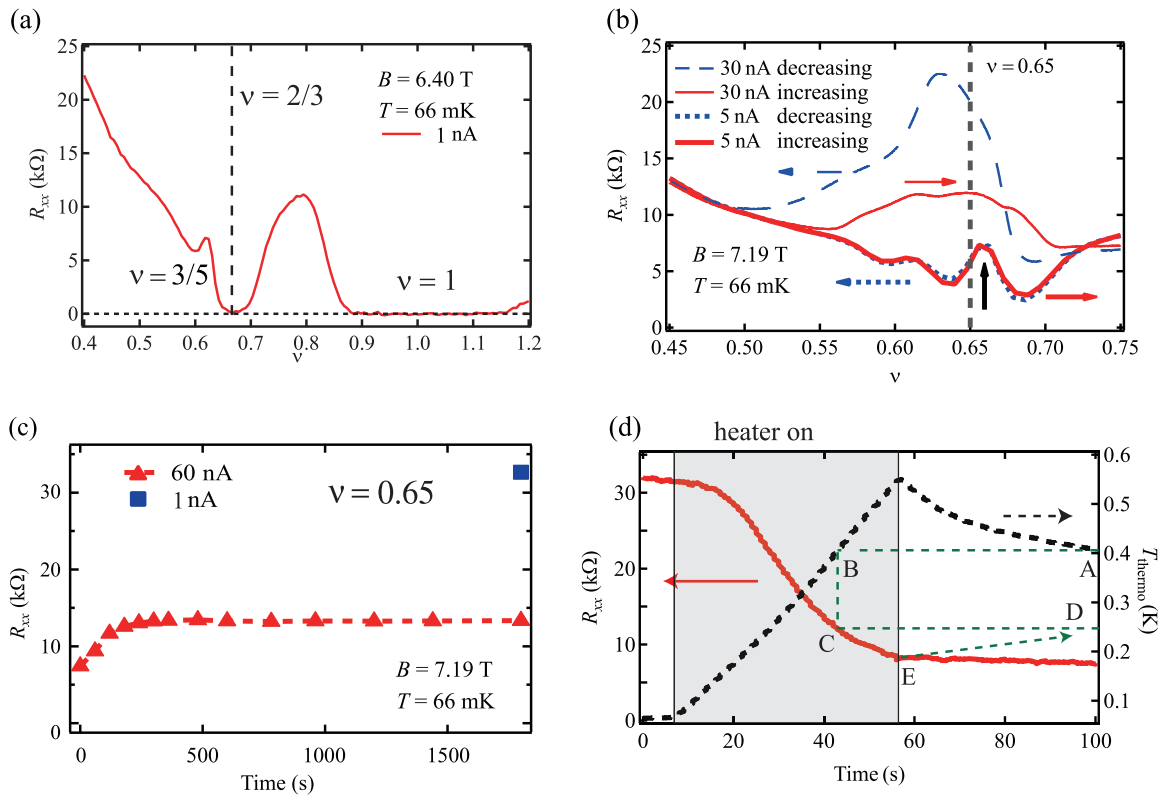


FIG. 1. (a) Plot of R_{xx} versus ν in the vicinity of the $\nu = \frac{2}{3}$ unpolarized QHS. (b) Plot of R_{xx} versus ν in the region of $\nu = \frac{2}{3}$ QHS, including the phase transition point between the spin polarized and unpolarized states. The thick red (blue dotted) line represents a fast sweep of $d\nu/dt = 1 \times 10^{-2} \text{ s}^{-1}$ from a lower (higher) to a higher (lower) ν , which is realized by changing the electron density at a current of 5 nA. The maximum R_{xx} (indicated by the up arrow) corresponds to the phase transition point. The spin polarized and unpolarized $\nu = \frac{2}{3}$ QHSs are observed at the left and right sides of the maximum, respectively. The thin red (broken blue) line represents a slow ν sweep of $d\nu/dt = 1 \times 10^{-4} \text{ s}^{-1}$ in the increasing (decreasing) direction at a current of 30 nA. We find a clear hysteresis in R_{xx} . (c) Time evolution of R_{xx} at the $\nu = 0.65$ point and for a current of 60 nA. After pumping, decreasing the current to 1 nA yields an increase in R_{xx} of a factor of 2 (blue square point). (d) Time evolution of R_{xx} of the HLR and thermometer temperature T_{thermo} with the addition of a heating power of 1 mW for 50 s. The measuring current for R_{xx} is 1 nA. The red solid and black dotted lines represent the values of R_{xx} and T_{thermo} , respectively. (The green dotted lines and points A–E relate to Fig. 3.)

DNBP [Fig. 1(d)]. The measurement current is changed from a 60 nA pumping current for DNBP to 1 nA, in order to prevent the self-heating effect. The resistance is found to decrease with increasing temperature. However, there is a possibility of a substantial disagreement between the temperature measured by the thermometer T_{thermo} and the actual sample temperature T_{sample} . The sample, heater, and thermometer are at a distance of approximately 1 cm from each other in the dilution refrigerator mixing chamber. As T_{thermo} begins to decrease when the heater power is switched off [Fig. 1(d)], we suspect that rapid heating leads to a highly inhomogeneous temperature distribution in the mixing chamber, which is the reason for the difference between T_{sample} and T_{thermo} . Accordingly, we investigate the relationship between heating time and T_{sample} using R_{xx} at $\nu = \frac{1}{3}$ QHS.

First, we heat the mixing chamber with a heating power of 1 mW and measure the time evolution of R_{xx} at $\nu = \frac{1}{3}$ QHS. The filling factor is offset slightly from $\nu = \frac{1}{3}$ as the temperature sensitivity of the magnetoresistance remains high at low temperature [point X, Fig. 2(c) inset]. Consequently, we obtain R_{xx} as a function of heating time, i.e., $R_{xx}(t)$, and confirm the reproducibility of the time evolution of $R_{xx}(t)$ by repeating the same procedure [Fig. 2(a)]. Next, the relationship between R_{xx} and T_{sample} at $\nu = \frac{1}{3}$ QHS is obtained by slowly cooling the sample, while maintaining thermal equilibrium [Fig. 2(b)]. Using the two dependencies of the R_{xx} on the heating time and the T_{sample} at $\nu = \frac{1}{3}$ QHS, we obtain $T_{\text{sample}}(t)$ as a function of heating time t [Fig. 2(c)].

We convert the $R_{xx}(t)$ in Fig. 1(d) using the relationships determined above and obtain the T_{sample} dependence of R_{xx} in the HLR [Fig. 2(d)]. We recognize that R_{xx} decreases as the temperature increases ($dR_{xx}/dT < 0$) in the HLR. In a previous experiment [4], although a R_{xx} current dependence for $\nu = \frac{2}{3}$ QHS was reported, no negative temperature dependence was observed, because a strong DNBP induced by a large current was considered. This was to simultaneously offset the R_{xx} decrement owing to the heating in the high-current measurements. There are two possible explanations for the temperature dependence in the present study, one is that the NSP rapidly relaxes owing to the temperature increase, and the other is the intrinsic thermal property of the HLR.

To determine which explanation is more appropriate, we measure the relaxation speed at high temperature. Figure 3(a) shows the time evolution of the R_{xx} of the HLR for three different heating durations of 1 mW (0, 27, and 50 s) with a measuring current of 1 nA after 60 nA pumping for 1800 s; the T_{thermo} evolution is shown in Fig. 3(b). The red solid, green broken, and blue dotted lines in Fig. 3(a) represent the heating durations of 0, 27, and 50 s, respectively. At 66 mK, R_{xx} decreases by 6.8% for 90 s after DNBP. In this experiment, as the NSP is pumped by a larger current and for a longer period of time than previously, the NSP is expanded from the quantum well to the other layer by diffusion, and the NSP relaxation time is longer than in our previous experiments [12,13]. Moreover, after heating for 27 and 50 s, R_{xx} decreases by 16.2% and 12.7%, respectively, for 90 s.

However, these decreased values do not indicate the real value. The reduction is explained based on Fig. 1(d) as follows: (1) The temperatures of points A and B are the same; (2) as the sample and thermometer are almost in thermal equilibrium, the

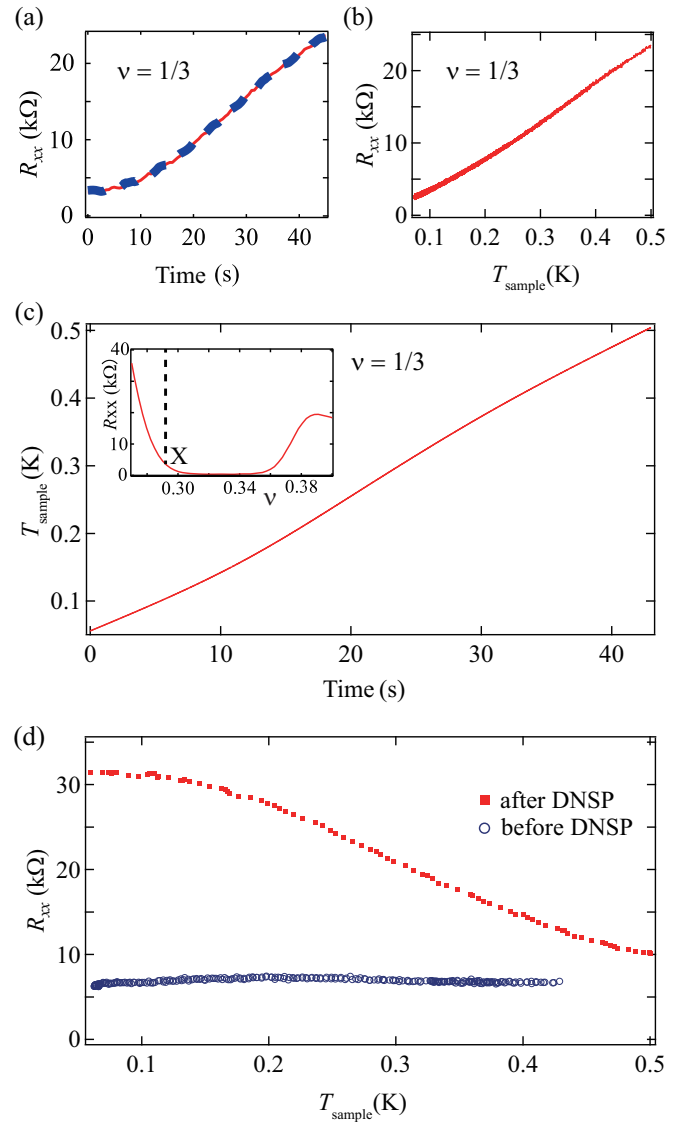


FIG. 2. (a) Time evolution of R_{xx} at $\nu = \frac{1}{3}$ QHS with additional heating power of 1 mW over 50 s. The filling factor is offset slightly from $\nu = \frac{1}{3}$ so that the temperature sensitivity of the magnetoresistance remains high at low temperatures [point X, inset of (c)]. The measuring current is 1 nA. The red solid and blue broken lines represent different data obtained by repeating the same procedure. The two lines are in perfect agreement with each other. (b) Relationship between R_{xx} and the sample temperature T_{sample} at $\nu = \frac{1}{3}$ QHS under thermal equilibrium. (c) $T_{\text{sample}}(t)$ obtained from (a) and (b). (d) T_{sample} dependence of R_{xx} at 1 nA. The blue circles denote the QHS data before DNBP, and the red squares denote the data after DNBP for an ac of 60 nA at 37.7 Hz. Notably, the data after DNBP exhibit a negative temperature dependence.

magnetoresistance of point C corresponds to the temperature at point B; (3) if there is no relaxation of the NSP, magnetoresistance is expected to change from point E to point D; and (4) the difference between the real magnetoresistance and the value at point D is the net decrease due to relaxation. From the results we deduce the relaxation time constant $\tau = 1290, 274,$ and 162 s at the average temperature values $T_{\text{ave}} = 66, 258,$ and 422 mK, respectively. The τT_{ave} value is almost constant,

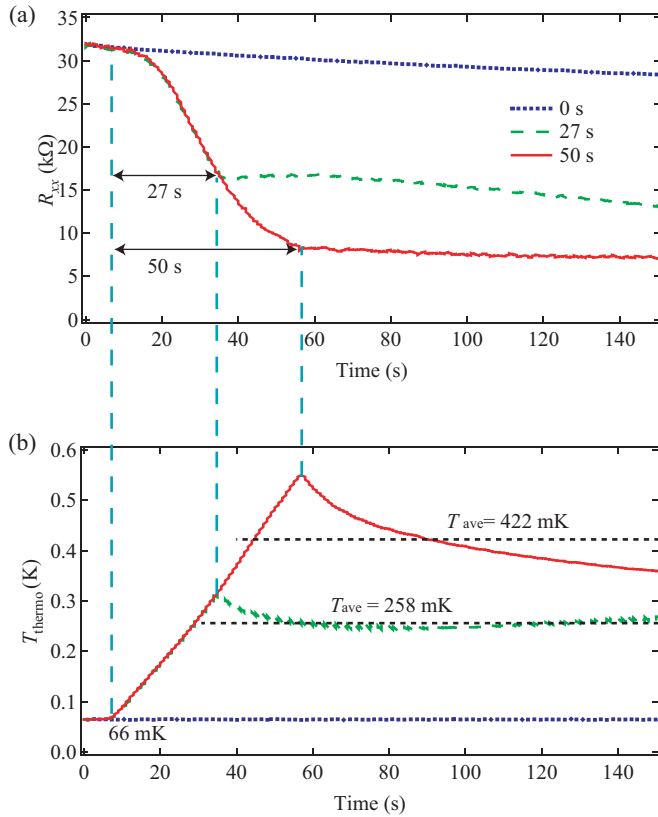


FIG. 3. (a) Time evolution of R_{xx} in HLR for three different heating durations (0, 27, and 50 s) at a measuring current of 1 nA after 60 nA pumping for 1800 s. Long-term pumping is used to reduce the spin diffusion effect [13]. (b) T_{thermo} evolution.

as if it satisfies a Korringa relation. Since the quantum Hall state is incompressible, the Korringa mechanism cannot be realized at least inside the domains. However, a Korringa-like mechanism may be possible at the domain boundary where the spin split energy is small [17].

If we assume that the decrease in R_{xx} between the heater-on-time (50 s) is caused by the relaxation, the relaxation time is 37 s, which is 4.4 times faster than that at 422 mK. Therefore, the decrement of R_{xx} from 66 mK to approximately 422 mK cannot be attributed to the increment in the relaxation rate.

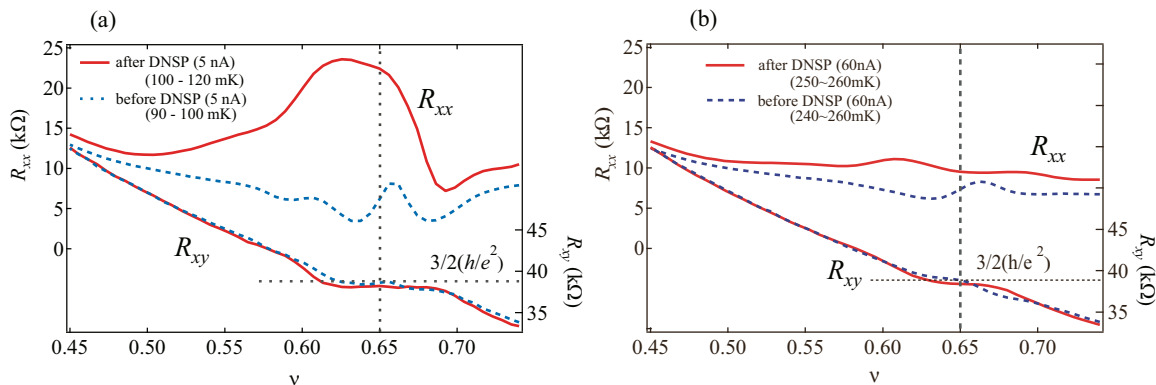


FIG. 4. R_{xx} (left axis) and R_{xy} (right axis) before and after DNSP as functions of ν for measuring currents of (a) 5 nA and (b) 60 nA. The broken vertical line indicates the value of ν at which DNSP is induced.

Hence, we conclude that the temperature dependence shown in Fig. 2(d) is mainly governed by the intrinsic thermal property of the HLR state. On the other hand, the HLR state pumped at the polarized $\nu = \frac{2}{3}$ QHS also exhibit a negative temperature dependence.

B. Filling factor dependence

In order to investigate the relationship between the QHS and HLR, we measure the filling factor dependence of the Hall resistance and the magnetoresistance. The R_{xx} and R_{xy} values before and after DNSP are plotted for measuring current values of 5 and 60 nA for a fast ν sweep with $d\nu/dt = 1 \times 10^{-2} \text{ s}^{-1}$. Figure 4(a) shows the plots of the data for low measuring current of 5 nA. The quantized Hall plateau is clearly seen only in the data before DNSP but the data after DNSP ($0.62 \leq \nu \leq 0.69$). Figure 4(b) shows the same data for a higher measuring current of 60 nA. We notice that the plateaus of the Hall resistance of both states are broken.

Next, we estimate the sample temperature in Fig. 4. As the heat capacity of the sample is very small (10^{-18} J/K [18], and the thermal boundary resistance is very high [19], the sample temperature changes quickly with the input power without a change in the environmental liquid helium temperature. The temperature corresponding to the power $P = RI^2$ is calibrated by the $\nu = \frac{1}{3}$ QHS, similar to the procedure in Fig. 2. As a result, the temperatures corresponding to the data after DNSP (60 nA) and before DNSP (60 nA) in Fig. 4(b) are 250–260 mK and 240–260 mK, respectively. We note that Kronmüller *et al.* [4] reported that the quantized R_{xy} disappears in the HLR state; however, they measured the R_{xy} via high current. From our experimental results, their experiment can explain that the disappearance of the quantized Hall resistance is caused by current heating. The magnetoresistance of the HLR state at $\nu = 0.65$ is smaller than that of Fig. 2(d). The reason is thought to be that the HLR state decreased more rapidly because of the filling factor sweep.

For almost the entire range of ν values ($0.51 \leq \nu \leq 0.71$, except in the region of $\nu = 0.66$) before DNSP, the R_{xx} at 5 nA (90–120 mK) is less than that at 60 nA (240–260 mK). This difference in R_{xx} corresponds to the positive temperature dependence that is a thermal property of metal. However, after DNSP, the R_{xx} at 5 nA (100–120 mK) is greater than that at

60 nA (250–260 mK), and the differential coefficient of R_{xx} with respect to the temperature takes on negative values for $0.5 \leq \nu \leq 0.68$.

IV. DISCUSSION

A. Longitudinal conductivity

First, we discuss the temperature dependence of the longitudinal conductivity σ_{xx} , which is expressed as $\sigma_{xx} = \rho_{xx}/(\rho_{xx}^2 + \rho_{xy}^2)$, where ρ_{xx} and ρ_{xy} are the longitudinal and Hall resistivities, respectively. Typically, σ_{xx} has an inverse temperature dependence to ρ_{xx} . However, because ρ_{xy} is larger than ρ_{xx} in our measured results, σ_{xx} exhibits a negative temperature dependence similar to ρ_{xx} (Fig. 5). In the ordinary QHS, both σ_{xx} and ρ_{xx} are minimal at 0 mK and have a positive temperature dependence (Fig. 5). Therefore, it is unusual for the HLR state to be explained by a property of the conductive electron state that completely satisfies the Landau levels in the magnetic field.

B. Similar phenomena

We refer to other experimental phenomena corresponding to $dR_{xx}/dT < 0$ in 2DES. We first consider the integer QHSs, which exhibit similar energy degeneration of different spin states to that for $\nu = \frac{2}{3}$ QHS. Previous studies have reported negative temperature dependence of the magnetoresistance bump amplitude ΔR_{bump} for integer QHSs [20,21]. In those studies, the ratio of the total magnetic field to the perpendicular magnetic field was varied by tilting the field, leading to the degeneration and domain formation of different spin states in the samples. The small ΔR_{bump} increases with temperature up to a certain critical temperature T_m , beyond which ΔR_{bump} decreases. The mechanism for this temperature dependence is considered to be related to the dissipation of the electric current at the domain walls. However, from experimental reports [22], the Hall resistivity deviates significantly from the quantized value at the spin transition point in integer QHSs, which is not the case in our experiment, in which the deviation is approximately 1%. Notably, the R_{xx} value at the spin transition point in an integer QHS [20] monotonically

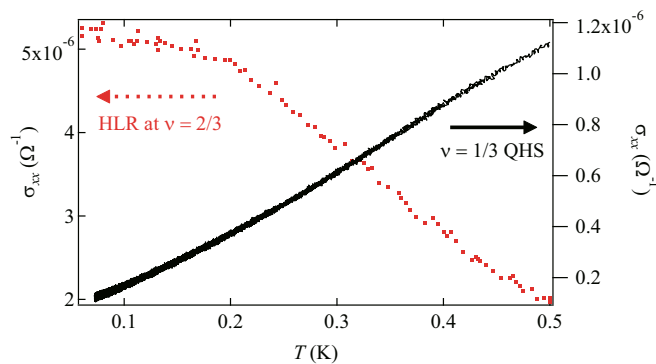


FIG. 5. Temperature dependence of longitudinal conductivity σ_{xx} at $\nu = \frac{1}{3}$ QHS and for HLR at $\nu = \frac{2}{3}$ QHS. The black solid line and red dots correspond to the $\nu = \frac{1}{3}$ QHS and HLR at $\nu = \frac{2}{3}$ QHS, respectively. The longitudinal conductivity is obtained as $\sigma_{xx} = \rho_{xx}/(\rho_{xx}^2 + \rho_{xy}^2)$.

increases with temperature, unless the base R_{xx} value is subtracted. Therefore, the temperature dependence of the total magnetoresistance of the integer QHS is positive and completely opposes the negative temperature dependence of our data.

Next, we refer to even-denominator states with filling factor $\nu = \frac{9}{2}$ and a small number of higher half-odd integer values [23–26], which indicate negative temperature dependence [23,24]. The HLR state and the even-denominator state are similar not only because of their negative temperature dependence, but also because of the following properties: (1) The magnetoresistance becomes of the same order as the Hall resistance value with decreasing temperature, but it is several times smaller; and (2) the Hall resistance of the HLR state takes the quantized Hall resistance value, while the even-denominator state takes the Hall resistance value corresponding to the electron density and the magnetic field [23,24]. The negative temperature dependence can be explained by the long-range ordering of the nematic liquid state [27–29].

C. Model of HLR state

1. Possible structure

Next, based on similar phenomena reported in the referenced experimental results, we develop a speculative model of the HLR state. It is difficult to explain both the quantized Hall resistance and the large negative temperature dependent magnetoresistance by means of a uniform phase, as can be inferred from the discussion in Sec. IV A. On the other hand, there is no direct correspondent state to the HLR state in the referenced phenomena. Nevertheless, it is noteworthy that the resistances of the even-denominator states with filling factor $\nu = \frac{9}{2}$ and others are large and exhibit negative temperature dependence, as discussed in Sec. IV B [23,24]. Moreover, the Hall resistance of the even-denominator states takes on classical values. In addition, the anisotropy in the hysteretic transport suggests that the domain structure has a unidirectional form [12]. Therefore, it is possible that the HLR has a stripe-shaped domain structure arising from the polarized and unpolarized $\nu = \frac{2}{3}$ QHSs. (We call our model the “stripe-shaped domain structure” to distinguish it from the charge density stripe model. The stripe-shaped domain structure constructed by the polarized and unpolarized phases is essentially different from the even-denominator states of $\nu = \frac{9}{2}$, etc., which are constructed by different electron-density zones with the same spin state [27].) When the electric current crosses the domains, the electrons encounter obstacles and the Hall resistance exhibits quantized values since the stripe-shaped domain also has the same $\nu = \frac{2}{3}$ filling factor but a different spin state.

The negative temperature dependence of the HLR state cannot be explained by the long-range order of the nematic liquid crystal [28,29]. The conductivity of the HLR state should be explained by the hopping conductance across the stripe-shaped domain with different spin states. The negative temperature dependence of the HLR state can be explained as follows: (1) the hopping conductance increases owing to the increases in temperature; and (2) the stripe-shaped structure is broken owing to the increase in temperature and the resistance decreases by collapse of the obstacle, and the stripe-shaped is

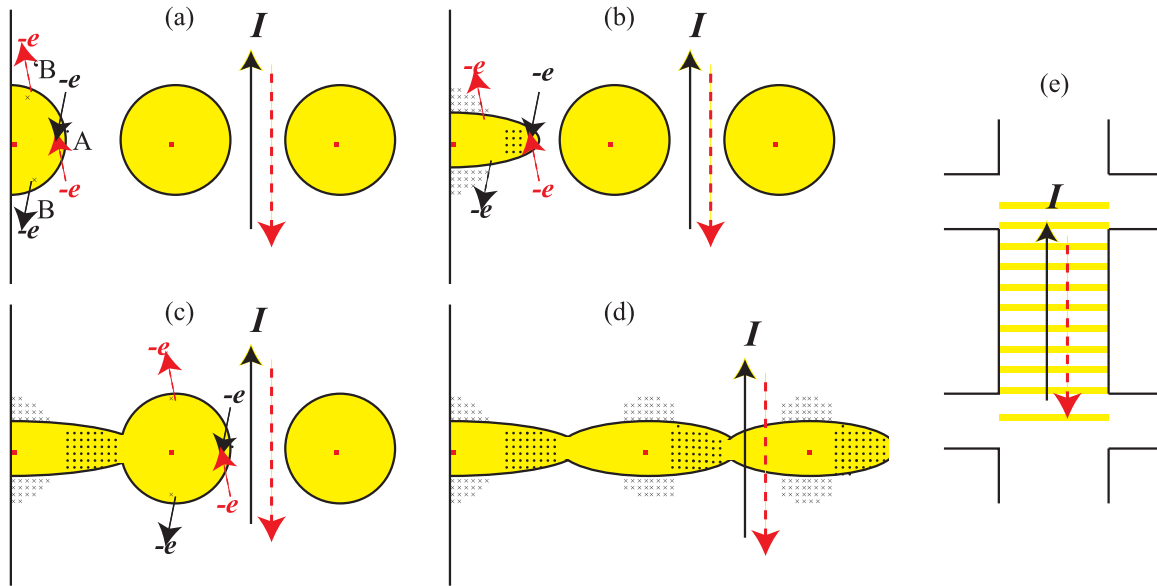


FIG. 6. Model of HLR state construction. (a) Initial domain structure. The left side is the edge of the sample. The red squares indicate disorder and the yellow circles are the puddle domains constructed from the polarized QHS affected by the disorder potential. We assume that the electrons enter the puddle domain from position A and exit the domain at the B or B' position. The black solid arrows indicate the case of the upper direction ac current, and the red dotted arrows indicate the reverse case. The electron flips the nuclear spin to the magnetic field direction (black closed circle) at A and to the direction opposite the magnetic field (black cross) at B and B'. (b) From the nuclear polarization, the puddle domain deforms the shape shown in the figure. (c) The puddle domain connects with neighboring puddle domains. (d) The puddle domains connect with each other, forming a stripe-shaped structure. (e) Schematic diagram of the Hall bar in the HLR state.

recovered reversibly owing to the decrease in temperature, while the nuclear polarization lasts. We cannot determine which one is a major factor from our present data.

2. Construction process

Next we try to conjecture a stripe-shaped domain construction process of the HLR. Before DNSP, the unpolarized QHS domain is dominant, and a “puddle” domain is constructed by the polarized QHS at $\nu = 0.65 < \frac{2}{3}$ [11]. When the puddle domain covers the edge, the electric current leaves from the sample edge. An electron passing through the domain boundary jumps into the puddle domain from the main domain [17]. When the electron passes through the domain boundary, the electron spin flips and, simultaneously, so too does the nuclear spin [point A of Fig. 6(a)]. When the electron goes away from the the puddle domain through the domain boundary, the electron spin flips to the reversible direction and, simultaneously, so too does the nuclear spin [point B and B' of Fig. 6(a)].

As a result, the nuclear spin field increases the total magnetic field and the puddle domain area increases in the cross direction of the electric current [Fig. 6(b)]. The nuclear spin field decreases the total magnetic field and the puddle domain area decreases at this point of the domain boundary. Assuming that the puddle domain expands in a direction orthogonal to the current direction and contracts in a direction parallel to the current direction, the puddle domains connect. This leads to the construction of a stripe-shaped domain structure [Figs. 6(d) and 6(e)].

Hayakawa *et al.* [30] observed the length scale of the initial domain formation near the spin transition point of $\nu = \frac{2}{3}$ QHS

to be approximately $3 \mu\text{m}$, using the optical method. This initial domain formation is governed by the interplay between the exchange interaction and disorder potentials, which are primarily created by charged donors in the remote doping layer and have a length of approximately $1 \mu\text{m}$ [30]. Our sample is very similar to the sample examined in that study in terms of mobility and structure. Because the disorder potentials likely affect the domain formation after DNSP, we consider the scale of the HLR state domain formation to be of the same order as the scale of the disorder potentials. Thus, the the puddle domains change the shape and connect each other. To confirm the construction of this domain structure, the domain structure in the HLR state must be observed using optical methods. Preliminary results have been obtained and the stripe-shaped domains have been observed [31,32].

V. SUMMARY

We measured the temperature dependence of the enhanced R_{xx} value caused by DNSP pumping at $\nu = \frac{2}{3}$ QHS. By dividing the pumping current and measuring current and quickly changing the sample temperature, we found that the enhanced resistance state exhibited a negative temperature dependence and a quantized Hall resistance plateau. This temperature dependence was discussed on the basis of a stripe-shaped domain structure consisting of polarized and unpolarized phases.

ACKNOWLEDGMENTS

We are thankful to N. Kumada, K. Muraki, and Y. Hirayama for not only providing us with a high mobility sample but also for many fruitful discussions. We

are also grateful to G. Yusa, S. Takagi, Z. F. Ezawa, N. Shibata, H. Akera, T. Okamoto, Y. Sasaki, and K. Iwata for useful discussions. This research was supported in part by JSPS KAKENHI, Grants No. 24540319, No. 24540331, and

No. 15K05135, MEXT KAKENHI, Grants No. 25103722, and a Grant-in-Aid for the Global COE Program “The Next Generation of Physics, Spun from Universality and Emergence.”

-
- [1] Z. F. Ezawa, *Quantum Hall Effects, Field Theoretical Approach and Related Topics*, 2nd ed. (World Scientific, Singapore, 2008).
- [2] S. M. Girvin and A. H. MacDonald, *Perspectives in Quantum Hall Effects*, edited by A. Pinczuk and S. Das Sarma (Wiley, New York, 1997).
- [3] J. P. Eisenstein, H. L. Stormer, L. N. Pfeiffer, and K. W. West, *Phys. Rev. B* **41**, 7910 (1990).
- [4] S. Kronmüller, W. Dietsche, J. Weis, K. von Klitzing, W. Wegscheider, and M. Bichler, *Phys. Rev. Lett.* **81**, 2526 (1998).
- [5] S. Kronmüller, W. Dietsche, K. von Klitzing, G. Denninger, W. Wegscheider, and M. Bichler, *Phys. Rev. Lett.* **82**, 4070 (1999).
- [6] K. Hashimoto, K. Muraki, T. Saku, and Y. Hirayama, *Phys. Rev. Lett.* **88**, 176601 (2002).
- [7] N. Kumada, K. Muraki, and Y. Hirayama, *Science* **313**, 329 (2006).
- [8] L. Tiemann, G. Gamez, N. Kumada, and K. Muraki, *Science* **335**, 828 (2012).
- [9] N. Kumada, D. Terasawa, Y. Shimoda, H. Azuhata, A. Sawada, Z. F. Ezawa, K. Muraki, T. Saku, and Y. Hirayama, *Phys. Rev. Lett.* **89**, 116802 (2002).
- [10] O. Stern, N. Freytag, A. Fay, W. Dietsche, J. H. Smet, K. von Klitzing, D. Schuh, and W. Wegscheider, *Phys. Rev. B* **70**, 075318 (2004).
- [11] S. Kraus, O. Stern, J. G. S. Lok, W. Dietsche, K. von Klitzing, M. Bichler, D. Schuh, and W. Wegscheider, *Phys. Rev. Lett.* **89**, 266801 (2002).
- [12] K. Iwata, M. Morino, A. Fukuda, N. Kumada, Z. F. Ezawa, Y. Hirayama, and A. Sawada, *J. Phys. Soc. Jpn.* **79**, 123701 (2010).
- [13] M. H. Nguyen, S. Tsuda, D. Terasawa, A. Fukuda, Y. D. Zheng, and A. Sawada, *Phys. Rev. B* **89**, 041403 (2014).
- [14] K. Muraki, N. Kumada, T. Saku, and Y. Hirayama, *Jpn. J. Appl. Phys.* **39**, 2444 (2000).
- [15] K. Hashimoto, K. Muraki, N. Kumada, T. Saku, and Y. Hirayama, *Phys. Rev. Lett.* **94**, 146601 (2005).
- [16] J. G. S. Lok, S. Kraus, O. Stern, W. Dietsche, K. von Klitzing, W. Wegscheider, M. Bichler, and D. Schuh, *Physica E* **22**, 138 (2004).
- [17] T. Jungwirth and A. H. MacDonald, *Phys. Rev. Lett.* **87**, 216801 (2001).
- [18] V. Bayot, E. Grivei, S. Melinte, M. B. Santos, and M. Shayegan, *Phys. Rev. Lett.* **76**, 4584 (1996).
- [19] J. Amrit and J. P. Thermoau, *J. Phys. Conf. Ser.* **150**, 032002 (2009). We refer to the Kapitza resistance data for Si because no data exist for GaAs.
- [20] E. P. De Poortere, E. Tutuc, and M. Shayegan, *Phys. Rev. Lett.* **91**, 216802 (2003).
- [21] K. Toyama, T. Nishioka, K. Sawano, Y. Shiraki, and T. Okamoto, *Phys. Rev. Lett.* **101**, 016805 (2008).
- [22] T. Okamoto, K. Sasaki, K. Toyama, R. Masutomi, K. Sawano, and Y. Shiraki, *Phys. Rev. B* **79**, 241302 (2009).
- [23] M. P. Lilly, K. B. Cooper, J. P. Eisenstein, L. N. Pfeiffer, and K. W. West, *Phys. Rev. Lett.* **82**, 394 (1999).
- [24] R. R. Du, D. C. Tsui, H. L. Stormer, L. N. Pfeiffer, K. W. Baldwin, and K. W. West, *Solid State Commun.* **109**, 389 (1999).
- [25] A. Endo, N. Shibata, and Y. Iye, *J. Phys. Soc. Jpn.* **79**, 103707 (2010).
- [26] A. A. Koulakov, M. M. Fogler, and B. I. Shklovskii, *Phys. Rev. Lett.* **76**, 499 (1996).
- [27] E. Fradkin, S. A. Kivelson, M. J. Lawler, J. P. Eisenstein, and A. P. Mackenzie, *Annu. Rev. Condens. Matter Phys.* **1**, 153 (2010).
- [28] E. Fradkin, S. A. Kivelson, E. Manousakis, and K. Nho, *Phys. Rev. Lett.* **84**, 1982 (2000).
- [29] E. Fradkin and S. A. Kivelson, *Phys. Rev. B* **59**, 8065 (1999).
- [30] J. Hayakawa, K. Muraki, and G. Yusa, *Nat. Nanotechnol.* **8**, 31 (2013).
- [31] J. Hayakawa, Doctoral dissertation, Tohoku University, 2011 (in Japanese).
- [32] After the submission, the stripe-shaped domain structure has been observed clearly by photoluminescence microscopy. (J. N. Moore, J. Hayakawa, T. Mano, T. Noda, and G. Yusa, Abstract of 21st International Conference on Electronic Properties of Two-Dimensional Systems 2015).